Polymer Testing 150 (2025) 108926

Contents lists available at ScienceDirect

Polymer Testing

journal homepage: www.elsevier.com/locate/polytest

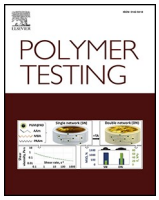

Effect of the morphology of hard segment domains in bio-based polyurethanes on the filtration properties of nanostructured filters

Simona Uhercova *, Dusan Kimmer, Muhammad Yasir, Lenka Lovecka, Miroslava Kovarova, Tomas Plachy, Vladimir Sedlarik **

Centre of Polymer Systems, University Institute, Tomas Bata University in Zlín, Třída Tomáše Bati 5678, 76001, Zlín, Czech Republic

ARTICLE INFO

Keywords:
Biomass
Synthesis of polyurethanes
Electrospinning
Nanofiber membrane
Air filtration

ABSTRACT

Renewable polymers have attracted significant attention in recent years as alternatives to fossil-based materials, driven by concerns about the depletion of such resources and the need for sustainable development. This study reports on the synthesis of polyurethanes from renewable biomass-derived diols, and their subsequent application in nanostructured air filters produced via electrospinning. Comparison is made of the properties of bio-based polyurethane samples that varied in the molecular weights of the inherent poly (1,3-propanediol) soft segments. Their physical-mechanical properties were analysed, along with the morphology and filtration performance of the nanostructures. It was found that the arrangement of the hard segments affected both phase temperature transitions (i.e. the glass transition and melting point) of the prepared polyurethanes. Positive effect hard segments domain arrangements and the best filtration properties were observed for a bio-polyether-based aromatic polyurethane prepared with molar ratio of diisocyanate:polyether polyol:chain extender of 4.7:1:3.7 and a molar mass of used renewable polyol 1000 g/mol, a nanostructure boasting the largest pore size of those tested. Filter with pressure drop of 49 Pa only possessed quality factor exceeding 0.045 Pa^{-1}. The work confirms the fact that the effects of fiber diameter and pore size on the filtration properties of nanostructured air filters fabricated to eliminate ultra-fine particles cannot be judged separately.

1. Introduction

The chemical industry is transitioning to renewable and sustainable plastics in response to economic and ecological concerns about the future usage of fossil raw materials [1]. This trend has been reflected in the adoption of polyurethane (PU), a form of plastic which can be varied to have wide-ranging properties and applications. Examples of the latter include types of glue and sealant, flexible and rigid foam, liquid paint and varnish, solutions employed in the manufacture of synthetic leather and thermoplastic elastomers (TPU) [2,3]. PU for filtration application is often chosen as a material composing a nanostructure due to its chemical stability, good chemical properties (first of all glass transition temperature – Tg), excellent nanofiber forming characteristic [4,5].

One of the main reasons for using PUs is that the properties of PU can vary in wide range, so it is possible to adjust them for many applications [6]. PU nanostructures have application in high-performance air filters, protective textiles, wound dressing materials, sensors and biomedical applications. PU can be mixed with other polymers and fillers e.g. carbon nanotubes [7,8].

Bio-based raw materials (e.g. 1,3-propanediol and 1,4-butanediol) have only been made commercially available at low cost with sufficient purity to synthesize PU for a short period of time [9]. Recent advances in bioprocessing [10–12] have also boosted the production of bio-based raw materials for the synthesis of PU, such as 1,4-butanediol (BD), succinic acid and adipic acid [10–13]. Great interest has been paid lately to PUs fabricated from bio-based materials since environmental resources are becoming ever more scarce [14–19]. Applying bio-based polyols in PU chemistry, therefore, affords the opportunity for sustainable and environmentally-friendly systems [20,21]. Bio polyols synthesized from bio-based 1,3-propanediol have been used, for instance, in the production of PU reactive hot-melt adhesive [22]; the DuPont company also offers poly (1,3-propanediol) (PPD) as a 100 % renewable polyol [23]. Polyols constitute a key raw material in the fabrication of PUs, and are primarily produced from fossil-fuels, namely

* Corresponding author.
** Corresponding author.
E-mail addresses: s_dockalova@utb.cz (S. Uhercova), sedlarik@utb.cz (V. Sedlarik).

https://doi.org/10.1016/j.polymertesting.2025.108926
Received 24 February 2025; Received in revised form 15 June 2025; Accepted 11 July 2025
Available online 12 July 2025

petroleum, which has held back research on alternatives [24], although moves are afoot for a gradual shift from fossil-based to biomass-based polyols [25]. The latter can be synthesized from lignin [26], agricultural waste [27,28], vegetable oil [29–34] and other renewable resources. Elastomers formulated from bio-based PUs, wherein bio polyols constitute a raw material, are an example of a practical application that has garnered interest [35–39].

Thermoplastic polyurethane elastomers (TPU) are segmented polyadducts with a two-phase domain microstructure consisting of hard and soft segments [40–42]. The high modulus of TPU is attributable to hard block domains made from hard segments, which act as cross-linked, physically bonded crystalline centres dispersed in the soft segment of flexible polyol chains. The hard block domains, therefore, act as molecular reinforcing fillers. Another reason for researching the PPD diols comprised the fact that polyethers tend to be less compatible with 4, 4′-methylene-diphenyl diisocyanate (MDI) than polyester diols, hence TPU derived from them shows a higher degree of phase separation. Increasing the length (molecular weight) of the soft segment diols would promote domain separation too [24].

Polyether TPU is usually formulated from poly (oxytetramethylene) diols (polytetrahydrofuran). It was synthesized herein from renewable polypropylene diols with an identical content of hard segments (w_{HS} = 60 % by mass). The given concentration was informed by a prior study, wherein high modulus TPU with a maximum tested volume of hard segments (the molar ratio was MDI:polymeric diol:BD and equalled 9:1:8) exerted a positive influence on the efficiency of nanofiber formation in an electrostatic field [43]. The hard segment domains consisted of aligned chains of urethane groups interlinked by hydrogen bonds in three dimensions. With respect to PU samples prepared from bio-based 1,3-propanediol (PU 500) at a molar ratio of 2.5:1:1.5, almost an entirely alternating arrangement of hard and soft segments was expected, resulting in a material with numerous, small, evenly dispersed hard segments in the soft segment portions.

The first commercial PU fiber was developed in Germany in the early 1940s [2]. It was made by reacting hexamethylene diisocyanate with a slight excess of 1,4-butanediol. Elastic fibers commonly referred to as Spandex are the most notable with regard to mass production, and constitute a generic term approved by the US Federal Trade Commission.

An area of study that has recently proven popular concerns the development of air filtration materials capable of removing pollutants, especially dangerous nano-sized ones (particles up to 1 μm in size) [44–46]. Filters based on nanofibers with low fiber diameters have become more effective at eliminating ultra-fine particles, retaining low pressure drop of the filter [45,47]. The filtration properties of nanostructured materials fabricated by electrospinning are generally superior to those of filters prepared from meltblown materials [48]. Besides PU [49–53], fossil-based polymers frequently applied in the production of nanofibers in an electrostatic field include polyvinylidene fluoride (PVDF) [44,54], polyacrylonitrile (PAN) [55,56], polysulfone (PSU) [52,57], polyethersulfone (PESU) and polyamide (PA) [58,59].

The primary novelties of this work lie in i) synthesis of PU from renewable resources (bio-based diols) with addressing environmental and sustainability aspects, ii) finding optimal morphology of hard segments in tested PU which provides creation of bulky nanostructure with bigger pore sizes guaranteeing better air filtration performance with regard to the capture of ultra-fine particles in sizes from 20 nm to 400 nm in consequence of Brownian motion, iii) set up very efficient nanostructure via electrospinning for air filtration caused by arrangement of hard segments in bio-based PU. All of those novelties extend the desired level of filtration efficiency, pressure drop and thence quality factor.

2. Experimental

2.1. Materials

4,4′-methylene-diphenyl diisocyanate (MDI), bio-based polyether polyols (PPD 500, 1000, and 2000 g/mol), 1,4 butanediol (BD) and N, N-dimethylformamide (DMF) were purchased from Sigma-Aldrich (Germany). Sodium tetra-borate decahydrate (Borax) and citric acid were bought from PENTA (Czech Republic).

2.2. Preparation of the polymer solutions

PU samples were fabricated via a polyaddition reaction involving the diisocyanate, bio-based polyether diols (soft segment) and chain extender, by means of one-shot synthesis in DMF solvent; the content of hard segments (diisocyanates + chain extenders) was maintained at 60 % by mass. Prior to conducting such synthesis, the various PPD diols had been dried in a vacuum at 90 °C for ca 30 min. The MDI and BD were then added, and the reaction proceeded at 90 °C for 3–4 h. DMF was supplemented stepwise once the viscosity of the PU solution had started to increase. The concentrations (c) were adjusted to 18 %, 16 % and 15 % by mass respectively, corresponding to viscosities (η) from 2100 to 2400 mPa s, suitable for the electrospinning process. Electrical conductivity χ was increased to the value higher than 200 μS/cm by an addition of DMF solution (18.6 % by mass) of Borax and citric acid at the ratio of 1:3 for the electrospinning process. The samples of PU solutions for electrospinning process were prepared in molar ratios detailed jointly with resulting concentration, conductivity and viscosity in Table 1.

2.3. Fabrication of nanofibers

Nanostructures with a width of 40 cm were produced in an electrostatic field from the PU solutions on a SpinLine 40 electrospinning device (SPUR, Czech Republic), equipped with 32 fiber-forming nozzles arranged in two lines. The experimental conditions under which the PU nanofibers were spun comprised the following: an applied electric voltage of 75 kV; the distance between electrodes measured 20 cm; the polymer solution was dosed at 0.5 mL/min; the substrate movement rate was 0.2 m/min; the temperature equalled 23 ± 2 °C; and the relative humidity was 31 %. The nanofibers were deposited on polyethylene terephthalate or polypropylene nonwoven substrate, which lent mechanical support to the subsequent nanostructured filters. All the nanostructures of various thicknesses and surface areas were prepared under uniform electrospinning process conditions; thus, the parameters for fabrication were not individually optimized for each solution.

2.4. Characterization of the synthesized PU and prepared nanostructures

2.4.1. Fourier-transform infrared spectroscopy

Fourier-transform infrared attenuated total reflectance (FTIR-ATR) was employed to characterize the chemical composition of the prepared nanofibers (Nicolet iS5, Thermo Fisher Scientific, Waltham, USA); this occurred at the wavenumber range of 4000–400 cm^{-1}, 64 scans per spectrum and resolution of 4 cm^{-1}, with analysis in OMNIC software (Thermo Fisher Scientific, Waltham, USA).

2.4.2. Contact angle

The water contact angles (Θw) of the samples were gauged with adherence to EN 15802. Measurement was performed at laboratory temperature on a Surface Energy Evaluation System (Advex Instruments, Czech Republic), with evaluation of the data taking place in SeeSystem 7.0 software.

2.4.3. Differential scanning calorimetry

The thermal behavior of synthesized PU was determined by

Table 1
Properties of the synthesized PU solutions and thermoplastic PU (TPU) dry extracts.

Material marking[a]	Molar ratio	After synthesis		After adjustment for the electrospinning process			Content of renewable material (% by mass)
		c_S (% by mass)	η_S (mPa s)	c_{ES} (% by mass)	η_{ES} (mPa s)	χ (μS/cm)	
PU 2000	9:1:8	20	13200	18	2400	207	54.7
PU 1000	4.7:1:3.7	20	10640	16	2200	231	53.1
PU 500	2.5:1:1.5	20	4790	15	2100	242	50.4

[a] Compared samples possessed the same content of hard segments, i.e. 60 % by mass.

differential scanning calorimetry (DSC) on a DSC 1 STAR (Mettler Toledo, Switzerland) instrument. Measurements were recorded during such thermal analysis in an inert nitrogen atmosphere (50 mL/min) across a temperature range of 0–250 °C. The rate for heating and cooling was set at 10 °C/min.

2.4.4. Dynamic mechanical analysis

The viscoelastic properties of the PU samples were evaluated by dynamic mechanical analysis (DMA; DMA 1; Mettler Toledo) under tension mode. The linear viscoelastic region (LVE) was determined initially by performing an amplitude sweep. A temperature sweep followed, applying a strain within a range of the LVE region across temperatures of −80 to 40 °C, at a heating rate of 3 °C/min and frequency of 1 Hz. Glass transition temperatures (T_g) were obtained as peaks for viscous moduli (E''), since this approach corresponds well with the other thermal analyses employed to determine T_g.

2.4.5. Tensile tests

Tensile tests were conducted to determine values for tensile strength and Young's modulus on a Testometric universal machine (MT350-5CT); this happened in accordance with EN ISO 527 at a single-strain rate of 500 mm/min and room temperature. The specimens had been conditioned at 25 °C and 50 % relative humidity for 72 h before such testing took place. Each set of samples consisted of at least 5 specimens.

2.4.6. Scanning electron microscopy (SEM)

A Phenom Pro scanning electron microscope was used to examine the morphology of the material. In order to avoid an electrostatic charge accumulating during morphological observations, the surfaces of samples were sputter-coated with Au/Pd prior to the test. SEM was used to image electrospun fibers to observe the surface morphology and any defects, such as a bead in the structure, that might be incorporated during electrospinning and to determine the desired diameter of nanofibers. The electron beam was operated at an accelerating voltage of 10 kV. The mean diameter of fibers was measured via ImageJ version 1.52a software (National Institutes of Health and the Laboratory for Optical and Computational Instrumentation (LOCI, University of Wisconsin), Madison, Wisconsin (USA)).

2.4.7. Determination of porometry

Characteristics relating to the pore sizes of the membranes were assessed on a flow porometer (SPUR, Czech Republic) in accordance with ASTM F316-03 (2011); Galpor (Porometer, Belgium) was employed as a wetting liquid. Dry and wet tests were conducted on three circular samples cut out from the given materials and mean values were obtained for them. The resulting porosity measurements encompassed the mean pore diameters of the nanostructures and the maximum pore diameters; pore size distributions were counted as well.

2.4.8. Filtration efficiency

The filtration properties of samples were measured on a TSI 3160 fractional efficiency filter tester. The investigation took place at an aerosol NaCl flow rate of 30 L/min and a face velocity of 5.2 cm/s. The quality factor (quality filter, q_F) constituted an important parameter with regard to filtration performance, and was calculated by the following equation:

$$q_F = \frac{ln\,(1/P)}{\Delta p} \quad (1)$$

where P stands for penetration (P = 1 – E), E is efficiency and Δp is the pressure drop.

3. Results and discussion

3.1. Synthesis of PU solutions

"One-shot" way of PU synthesis was used for the preparation of PU solutions for submicron fiber forming process in electrostatic field. Process of polyaddition reaction with both bio polymeric diol and bio low molecular diol was very similar to reactions based on fossil diols with strictly difunctional monomers. Their purity from the viewpoint of functionality request was very high, content of used difunctional bio diols was higher than 99 %. Properties of prepared PU solutions after synthesis and after adjustment for fabrication in electrostatic are summarized in Table 1. Idealized chemical composition of synthesized PUs with the highest and lowest content of hard segments is represenseded in Fig. 1. Synthesized polyurethanes differed each other in hard segment morphology and length of soft segments.

3.2. Electrospinning process

Three various nanostructures were created from synthesized PU solutions despite the fact that all of them were fabricated under uniform electrospinning process conditions. Those differ first of all in nanofiber diameters and pore sizes. We suppose that nanofibers with lower fiber diameter will bemore flexible and create a formation with smaller pore sizes whereas nanofibers with higher fiber diameter will be tougher, more flexible and more reinforced structure with larger pore size will arise. Brownian motion dominantly affects the filtration efficiency in the area of ultrafine particles capture consequently higher nanostructure with larger pore sizes (bringing about lower pressure drop) can positively affect filtration performance [60–62]. Fig. 2 presents the idealized morphological arrangement of the hard segments in the tested PU structures.

3.3. Fourier transform infrared spectroscopy

The chemical structures of the bio-based PU nanofibers were analysed from FTIR spectra. As detailed in Fig. 3, all the spectra show peaks typical for an aromatic PU derived from a polyether diol. The vibration bands at 3312 and 1528 cm^{-1} correspond to -NH stretching, while the peaks in the region spanning 3000 to 2770 cm^{-1} relate to -CH responses to asymmetric and symmetric stretching vibrations. The wavenumbers at 1528 and 1222 cm^{-1} are attributed to frequencies of the -CN group, whereas the band at 1076 cm^{-1} pertains to symmetric -C-O-C- stretching. Confirmation that the monomers had reacted fully and appropriate polymerization conditions had transpired is provided by a peak absent from the curves at ca 2270 cm^{-1} that would otherwise represent free –NCO groups [60–62].

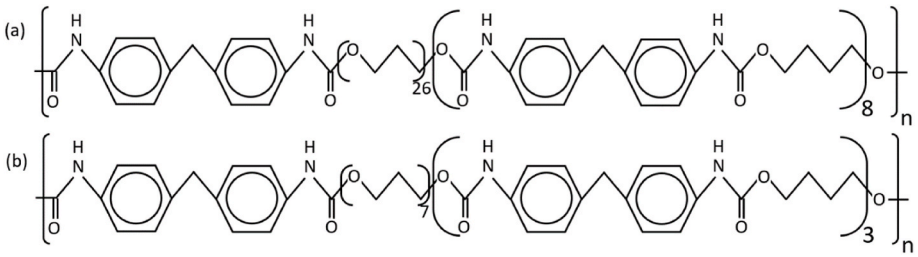

Fig. 1. Idealized chemical composition of synthesized PUs with the highest – PU 2000 (A) and lowest - PU 500 (B) content of hard segments.

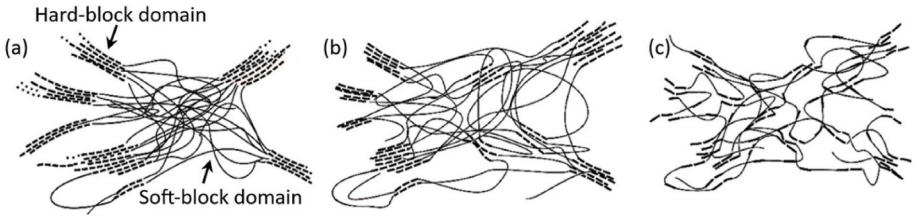

Fig. 2. Arrangement of hard segments in idealized structures of the synthesized PUs: (a) PU 2000, (b) PU 1000 and (c) PU 500.

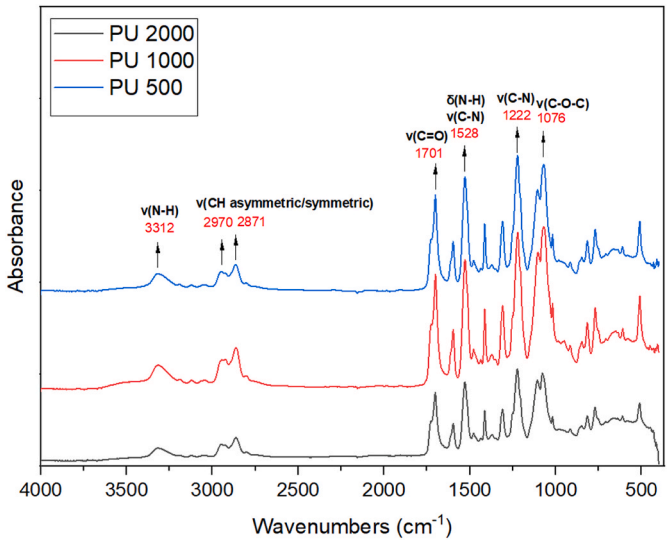

Fig. 3. FTIR spectra obtained in ATR mode for the tested PU materials.

3.4. Differential scanning calorimetry

Determining changes that occurred in the melting and crystallization temperatures permitted investigation by DSC of the morphology of hard segment domains and variation in the lengths of the soft segments in the PPD-derived, bio-based PU. Incorporating soft segment polyols that varied in molecular weight in the specimens, while maintaining a constant, uniform weight fraction of hard segments, yielded synthesized PU materials with melting temperatures (T_m) of between 141 °C and 214 °C, these outer values being recorded for PU 500 and PU 2000, respectively; PU 1000 had an intermediate melting temperature of approximately 178 °C (Table 2). As illustrated in Fig. 4a, this parameter rose in parallel with an increase in the molecular weight of the PPD applied, a phenomenon attributed to the arrangement of the hard segments (see Fig. 3). The broad endothermic peak observed for the PU 500 and 1000 samples could be explained by the limited extent of structural order within the hard segment domains. In contrast, the PU 2000 sample exhibited a more pronounced and intense double peak, indicating a greater degree of arrangement [63]. This heightened regularity in structure is also evidenced in Fig. 4b, where a crystallization peak appears at 116 °C for the PU 2000 specimen. The PU 1000 sample presents a double peak at 128 °C, indicating a reduction in such regularity in comparison with PU 2000. The absence of an exothermic peak in the PU 500 sample, however, suggests the existence of a highly disordered structure which would inhibit crystallization (see Fig. 4).

3.5. Contact angles

The hydrophilicity of the synthesized nanostructured materials was gauged through recording contact angle measurements. The nanostructured PU materials tended to exhibit hydrophilic properties, as indicated by the water contact angles observed below 60° (see Table 2). This indicates that the molecular weights of the polyether diols did not influence the hydrophilicity of the prepared PU samples.

3.6. Mechanical properties of the synthesized PU

3.6.1. Tensile test

The state of hard segment aggregation is affected by the soft segments present. Polyether diols tend to be less compatible with MDI than those in polyester, and TPU derived from them shows a higher degree of phase separation, hence hard segment domains are usually larger and more complex. Increasing the molecular weight of the given diol also favours domain separation.

A tensile test was conducted to evaluate the stiffness of the materials.

Table 2
Data on the physical-mechanical properties of the bio-based PU materials, obtained by measurement of contact angles, tensile testing, DSC and DMA.

Material designation	Θw (°)	Young's modulus (MPa)	Tensile strength (MPa)	Temperature of melting (°C)	Elastic modulus (MPa)	Glass transition temperature (°C)
PU 2000	51.0 ± 4.6	234.0 ± 19.9	28.5 ± 4.7	214	3520	−12.6
PU 1000	58.9 ± 2.5	135.9 ± 13.1	11.5 ± 2.5	178	3982	−35.7
PU 500	57.5 ± 4.1	168.5 ± 8.4	12.8 ± 1.2	141	3709	−58.2

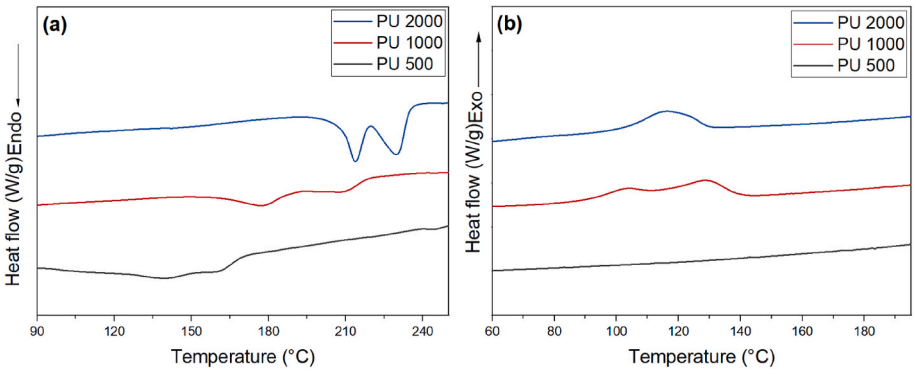

Fig. 4. DSC curves for the PU materials: (a) heating and (b) cooling.

Every PU sample contained the same concentration of hard segments, fixed at 60 % by mass. Their elevated hardness most likely arose from this uniformity in composition, made up of hard segments in large, well-defined domains. The PU 2000 specimen, as anticipated, exhibited the greatest stiffness, approximately 234 MPa. This was attributed to the superior arrangement of rigid segments within its polymer matrix. Moreover, it had the highest tensile strength. The PU 1000 and 500 samples demonstrated similar values to each other for Young's modulus and tensile strength, varying merely within standard deviation (Table 2); this finding was ascribed to the inadequate organization of hard segments within their structures. Arrangements of hard segments result to bulkier structure with larger pore sizes (PU 1000 – optimum structure from the filtration performance point of view) or on the contrary concise, less bulky structures with lower pore sizes (PU 2000 – large hard segments domains and PU 500 with spread hard segments, unreinforced, easy deformable structure). The measurement of filtration efficiency was done for NaCl particles in sizes 20 through 400 nm where Brownian motion dominantly effect the mechanism of particles capture.

3.6.2. *Dynamic mechanical analysis*

DMA confirmed the significant impact of precursor selection on the viscoelastic properties of the PU samples (Fig. 5). Applying polyether soft segments that differed in molecular weight and in the ratio of MDI: BD (although the mass content of hard segments was the same in each sample) resulted in PU systems with values for T_g of −58.2 °C, −35.7 °C and −12.6 °C, pertaining to the PU 500, 1000 and 2000 specimens, respectively (see Fig. 4a). These observations corresponded with the transition of polyether soft segments in the PU chains [64], since an increase in molecular weight reduced the extent of free volume, thereby significantly raising values for T_g [65].

Every sample was similar in terms of its elastic modulus (E' get about in the range from 3520 to 3982 mPa s) when in a glassy state (see Fig. 4b). Since the content of MDI and BD in each was comparable, the elastic modulus in this region was primarily determined by strong interactions of the isocyanate segments [63]. In the viscoelastic region, however, it was the influence of the polyol soft segments that predominated and directly altered the associated behaviour of the PU samples. Despite the PU 500 specimen exhibiting the lowest T_g and slowest decrease in E' values, the values recorded for it at room temperature exceeded those of every other PU sample. Notably, the softening process for the PU 2000 sample began at the highest temperature as it possessed the highest T_g, although the high mobility of its long polyol chains triggered a rapid drop in values for E'. It was concluded that the overall viscoelastic properties of the samples were strongly influenced by two factors: i. the arrangement of hard segments, and ii. the combination of their lengths of polyether soft segments and MDI: BD ratios.

3.6.3. *Scanning electron microscopy*

The morphology of the nanostructured layers was characterized by comparing SEM images at 5000 × magnification and measuring the diameters of nanofibers (see Fig. 6). The data obtained on the distribution of values for all the tested nanostructures were processed graphically. Despite the fact that the conditions for electrospinning and properties of the treated solutions were almost identical, differences in nanostructures existed. For example, the nanofibers of the PU 1000 sample were straight, thicker and more reinforced than elsewhere and constituted a nanostructure possessing larger pore sizes with low pressure drop. Nevertheless, the ultrafine particles exerting considerable Brownian movement are intercepted very effectively.

3.6.4. *Pore sizes*

The most critical aspects for the pore sizes of the nanostructures were thickness of nanostructure, basic weight, as well as the diameters and flexibility of the given nanofibers. These significantly affected certain parameters of the pores, as follows: i) average pore size diameter, ii)

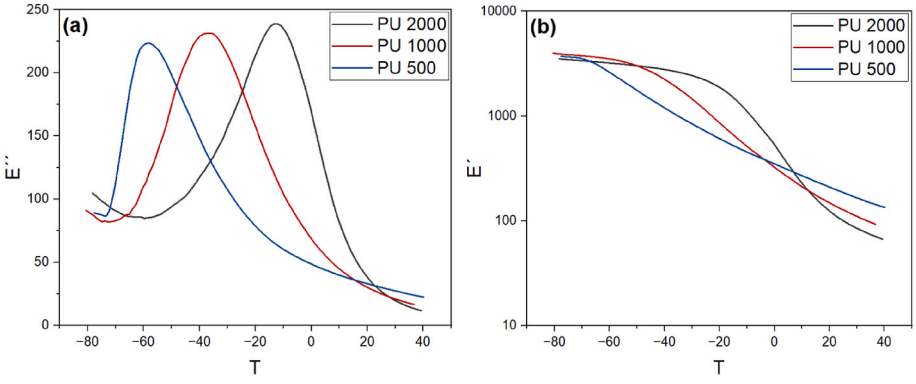

Fig. 5. DMA analysis of the prepared PUs: a) dependence of loss modulus on temperature and b) semi-log dependence of elastic modulus on temperature.

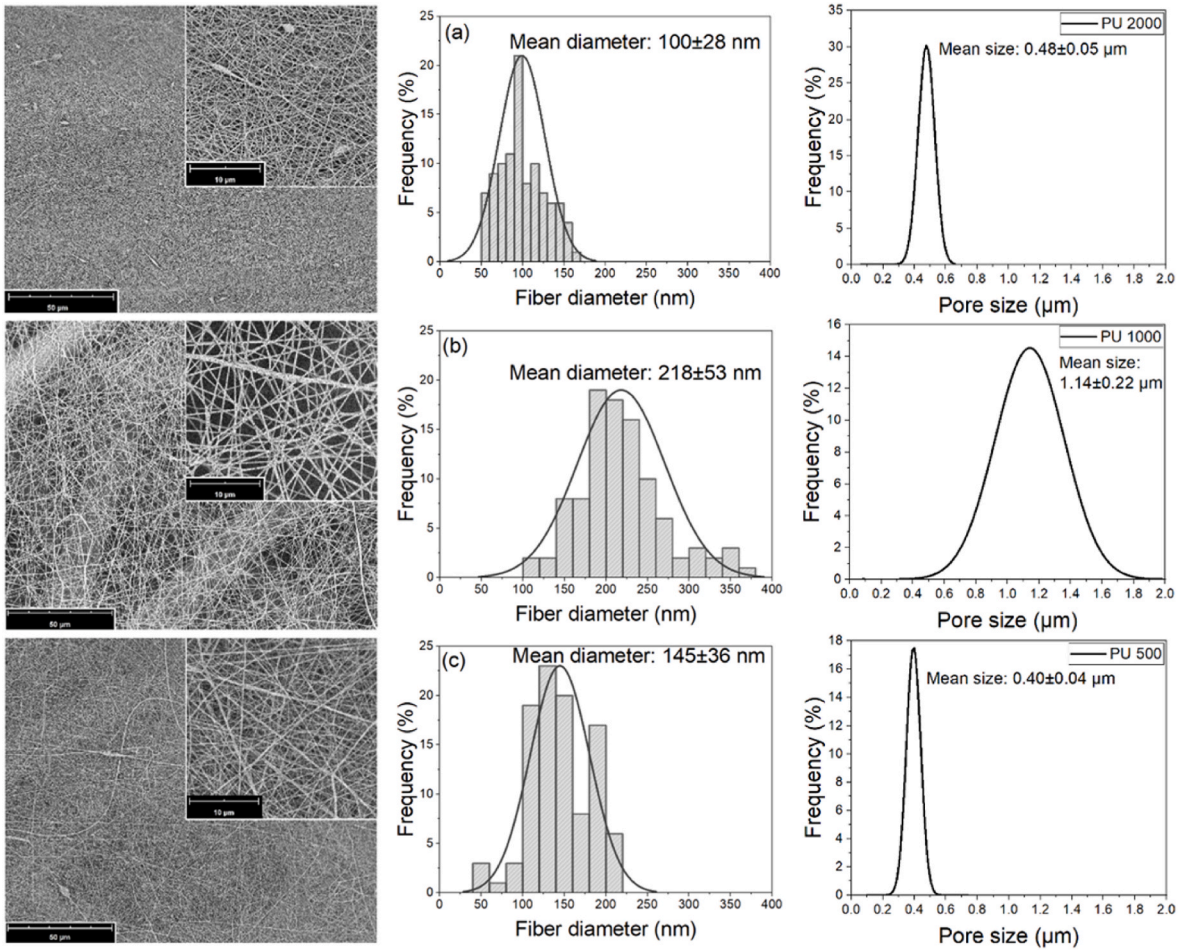

Fig. 6. Surface morphologies of the electrospun PU filters and their respective nanofibers, in addition to the pore diameter distributions of: a) PU 2000, b) PU 1000 and c) PU 500.

maximum pore size diameter; and iii) distribution of pore diameters. Each material was evaluated for its morphology and filtration performance. While PU 1000 possessed the lowest tensile strength and Young's modulus, its fiber diameter, average and maximum pore sizes, and associated distribution exceeded those of PU 2000 and PU 500 (see Table 3 and Fig. 6).

For confirmation of the effect exerted by the arrangements of hard segment domains on the pore sizes of the nanostructures and, consequently, filtration performance, values for the diameters of the nanofibers should be very similar or even identical.

3.6.5. *Filtration properties*

Three filters made of PU nanostructures based on bio PPD with variable molar weights are compared from the of filtration efficiency and quality factors point of view. With growing pressure drop, the filtration efficiency is increasing, while, in the case of recognition by means of quality factors with a growing pressure drop of filters, the q_F is partially decreasing.

To evaluate the filtration efficiency of tested filtration materials, a comparison of filters with the same values of pressure drops is necessary (Fig. 7a). The ones analysed had pressure drops of 111 Pa–118 Pa, with filtration efficiency rising in the sequence of PU 1000 > PU 2000 > PU 500. The PU 2000 nanofibers measured ca 100 nm in diameter (hence were more flexible in morphology), rendering them less than half the size of the PU 1000 equivalent. Cognate results were found for PU 500. Consequently, the average pore size for the PU 1000 nanostructure was much larger than for the PU 2000 and PU 500 nanostructures, with subsequent investigation evidencing its superior filtration performance. Further optimization of the properties of the nanostructures could be facilitated by changing the electrospinning conditions.

The significant differences in the pressure drops of the prepared filters complicated the comparison of their filtration properties, requiring a contrast of calculated quality factors instead (i.e. quality filters) to obtain such data [66]. The tendency for filtration presented in Fig. 7b was evidenced by evaluating this quality filter parameter at pressure drops in excess of 100 Pa (Fig. 8b) and below 100 Pa (Fig. 8a). The best findings in this regard were for materials with pressure drops of less than 100 Pa. Unfortunately, every filter fabricated from PU 500 demonstrated values greater than that, as the fiber-forming process in the electrostatic field was intense; thus, only the specimen with a minimal drop of 118 Pa is included in Fig. 8a.

The highest values for the aforementioned quality factor were obtained for filters derived from PU synthesized with PPD 1000 soft segments at the molar ratio of MDI:PPD:BD = 4.7:1:3.7 (see Fig. 9a and b). Nanostructures at this ratio resulted in samples that had a nanostructure morphology with a maximal pore size and the ability to capture ultrafine particles efficiently during Brownian motion. Filters showing

Table 3
Characterization of the nanostructures by SEM and porometry.

Material designation	Fiber diameter (nm)		Pore size (μm)	
	Mean	Min.-Max.	Mean	Maximum
PU 2000	100 ± 28	52 – 167	0.48 ± 0.05	0.62
PU 1000	218 ± 53	108–365	1.14 ± 0.22	1.84
PU 500	145 ± 36	59–211	0.40 ± 0.04	0.54

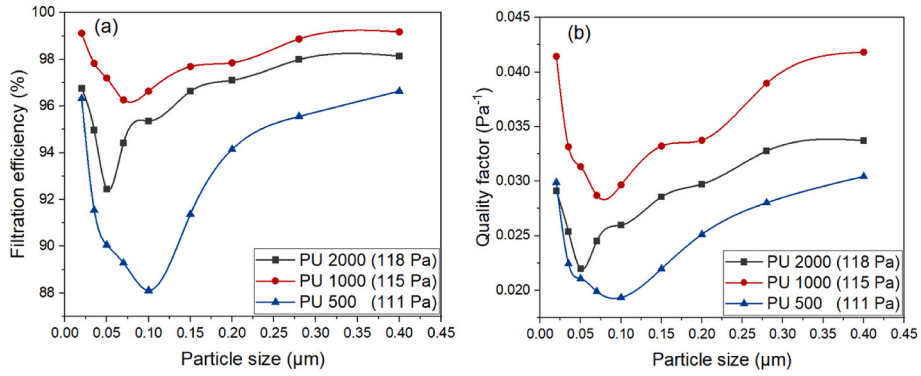

Fig. 7. Filtration performance of nanostructures with identical values for pressure drop, as fabricated from PU with the inclusion of organic PPD soft segments; evaluation of their a) filtration efficiency and b) quality factor.

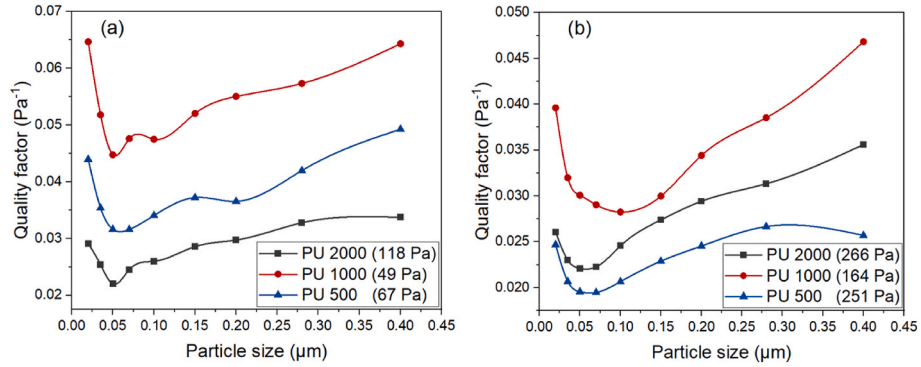

Fig. 8. Quality factors for selected filters with pressure drops lower than 100 Pa (a) and higher than 100 Pa (b).

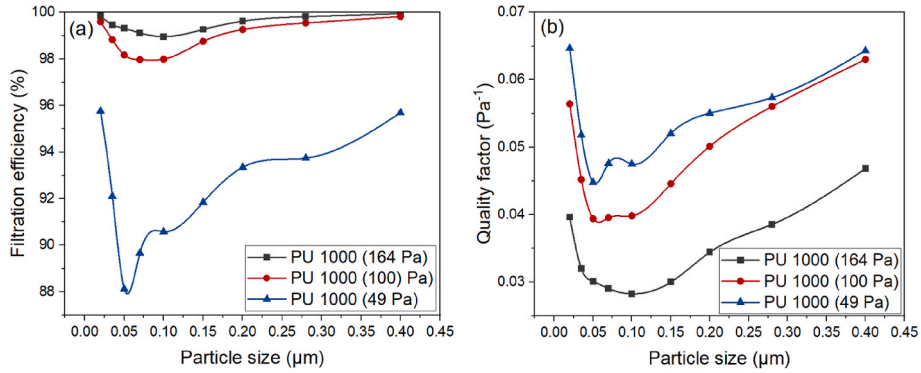

Fig. 9. Filtration efficiencies (a) and corresponding quality factors (b) for the best (PU 1000 derived) filters.

values for the quality factor (q_F) within the range of 30–70 kPa^{-1} demonstrated superior filtration properties.

Nanostructured layer (PU 1000) with high value of pore sizes (1.14 μm, Fig. 6b–Table 3), consequently low pressure drop (49 Pa, Fig. 8a) and high filtration efficiency in the area of ultrafine particles (Fig. 7a) are suitable with substantial benefit for combination with other micro-structured air filtration materials (e.g. melt blown) for improvement of capture efficiency of SARS-CoV-2 virus incurring coronavirus disease.

4. Conclusion

This study focused on synthesizing bio-based PU that contained various arrangements of hard segment domains and lengths of soft segments. The resulting materials were evaluated via a series of physical-mechanical tests. Although varying the lengths of the soft segments and the structural arrangements of hard segments did not affect the hydrophilicity of samples. It was discerned that thermal properties exerted a significant influence in this regard. With growing length of the PPD soft segment in PU chains the PU melting temperature is increasing and the glass transition temperature is decreasing. In spite of the fact that elastic moduli of synthesized PU were very similar in the range from 3520 to 3982 mPa s and fiber forming conditions in electrostatic field were the same, various nanostructures with distinct filtration properties were created, the effect of hard segment domains morphology and length of used soft segment being the reason. It proved impossible to judge separately the effects of fiber diameter and pore size on the filtration properties of nanostructured air filters fabricated to eliminate ultra-fine particles. The best filtration results were seen for materials prepared from PU with PPD soft segments at a molar weight of 1000 g/mol. Prepared, more effective nanostructure has been formed by

nanofibers with values of fiber diameter 218 ± 53 nm and mean pore size 1.14 ± 0.22 μm. Filters with pressure drops of 49 Pa merely possessed quality factor exceeding 0.045 Pa^{-1}.

CRediT authorship contribution statement

Simona Uhercova: Writing – original draft, Formal analysis, Data curation. **Dusan Kimmer:** Writing – original draft, Visualization, Validation. **Muhammad Yasir:** Formal analysis. **Lenka Lovecka:** Formal analysis. **Miroslava Kovarova:** Formal analysis. **Tomas Plachy:** Formal analysis. **Vladimir Sedlarik:** Supervision, Methodology, Funding acquisition, Conceptualization.

Declaration of competing interest

The authors declare the following financial interests/personal relationships which may be considered as potential competing interests: Vladimir Sedlarik reports financial support was provided by Ministry of Education Youth and Sports of the Czech Republic. Vladimir Sedlarik reports financial support was provided by Ministry of the Environment of the Czech Republic. Simona Uhercova reports financial support was provided by Tomas Bata University in Zlin. Vladimir Sedlarik reports financial support was provided by Tomas Bata University in Zlin. If there are other authors, they declare that they have no known competing financial interests or personal relationships that could have appeared to influence the work reported in this paper.

Acknowledgements

This work was supported from the European Just Transition Fund within the Operational Programme: Just Transition under the aegis of the Ministry of the Environment of the Czech Republic, project CirkArena number CZ.10.03.01/00/22_003/0000045 and Operational Programme Johannes Amos Comenius OP JAC "Application potential development in the field of polymer materials in the context of circular economy compliance (POCEK)", number CZ.02.01.01/00/23_021/0009004.

Authors are further grateful for co-funding from the development process of Centre of Polymer Systems, Tomas Bata University in Zlin, program DKRVO (RP/CPS/2024-28/002) supported by the Ministry of Education Youth and Sports of the Czech Republic. Muhammad Yasir also expresses his gratitude for support from the "Creativity, Intelligence & Talent for the Zlin Region" (CIT - ZK) programme. Simona Uhercová would also like to thank the Internal Grant Agency at Tomas Bata University in Zlin for its co-funding (project no. IGA/CPS/2024/003).

Data availability

Data will be made available on request.

References

[1] H. Sardon, D. Mecerreyes, A. Basterretxea, L. Avérous, C. Jehanno, From lab to market: current strategies for the production of biobased polyols, ACS Sustainable Chem. Eng. 9 (2021) 10664–10677, https://doi.org/10.1021/acssuschemeng.1c02361.

[2] G. Woods, The ICI Polyurethanes Book, JOHN WILEY & SONS, New York, n.d.

[3] G. Rossignolo, G. Malucelli, A. Lorenzetti, Recycling of polyurethanes: where we are and where we are going, Green Chem. 26 (2024) 1132–1152, https://doi.org/10.1039/D3GC02091F.

[4] W. Ma, W. Cao, T. Lu, R. Xiong, C. Huang, Multifunctional nanofibrous membrane fabrication by a sacrifice template strategy for efficient emulsion oily wastewater separation and water purification, J. Environ. Chem. Eng. 10 (2022) 108908, https://doi.org/10.1016/j.jece.2022.108908.

[5] C. Akduman, E.P.A. Kumbasar, Electrospun polyurethane nanofibers, in: F. Yilmaz (Ed.), Aspects of Polyurethanes, InTech, 2017, https://doi.org/10.5772/intechopen.69937.

[6] X. Pan, H. Wang, J. Wang, H. Wang, H. Shi, S. Wang, F. Ruan, Q. Feng, Composite thermoplastic polyurethane nanofiber membrane in waterproof and breathable application, Fibers Polym. 26 (2025) 2827–2837, https://doi.org/10.1007/s12221-025-00986-1.

[7] D. Kimmer, P. Slobodian, D. Petráš, M. Zatloukal, R. Olejník, P. Sáha, Polyurethane/multiwalled carbon nanotube nanowebs prepared by an electrospinning process, J of Applied Polymer Sci 111 (2009) 2711–2714, https://doi.org/10.1002/app.29238.

[8] A. Shaker, A.T. Khedewy, M.A. Hassan, M.A.A. El-Baky, Thermo-mechanical characterization of electrospun polyurethane/carbon-nanotubes nanofibers: a comparative study, Sci. Rep. 13 (2023) 17368, https://doi.org/10.1038/s41598-023-44020-x.

[9] T. Debuissy, P. Sangwan, E. Pollet, L. Avérous, Study on the structure-properties relationship of biodegradable and biobased aliphatic copolyesters based on 1,3-propanediol, 1,4-butanediol, succinic and adipic acids, Polymer 122 (2017) 105–116, https://doi.org/10.1016/j.polymer.2017.06.045.

[10] J. Bozell, G. Petersen, Technology development for the production of biobased products from biorefinery carbohydrates—the US department of Energy's "Top 10" revisited, Green Chemistry - GREEN CHEM 12 (2010), https://doi.org/10.1039/b922014c.

[11] J. Becker, A. Lange, J. Fabarius, C. Wittmann, Top value platform chemicals: bio-based production of organic acids, Curr. Opin. Biotechnol. 36 (2015) 168–175, https://doi.org/10.1016/j.copbio.2015.08.022.

[12] I. Bechthold, K. Bretz, S. Kabasci, R. Kopitzky, A. Springer, Succinic acid: a new platform chemical for biobased polymers from renewable resources, Chem. Eng. Technol. 31 (2008) 647–654, https://doi.org/10.1002/ceat.200800063.

[13] N.R. Barton, A.P. Burgard, M.J. Burk, J.S. Crater, R.E. Osterhout, P. Pharkya, B. A. Steer, J. Sun, J.D. Trawick, S.J. Van Dien, T.H. Yang, H. Yim, An integrated biotechnology platform for developing sustainable chemical processes, J. Ind. Microbiol. Biotechnol. 42 (2015) 349–360, https://doi.org/10.1007/s10295-014-1541-1.

[14] J.C. Khanderay, V.V. Gite, Fully biobased polyester polyols derived from renewable resources toward preparation of polyurethane and their application for coatings, J. Appl. Polym. Sci. 136 (2019) 47558, https://doi.org/10.1002/app.47558.

[15] D.V. Palaskar, A. Boyer, E. Cloutet, C. Alfos, H. Cramail, Synthesis of Biobased Polyurethane from Oleic and Ricinoleic Acids as the Renewable Resources via the AB-Type Self-Condensation Approach, Biomacromolecules 11 (2010) 1202–1211, https://doi.org/10.1021/bm100233v.

[16] C. Zhang, S.A. Madbouly, M.R. Kessler, Biobased polyurethanes prepared from different vegetable oils, ACS Appl. Mater. Interfaces 7 (2015) 1226–1233, https://doi.org/10.1021/am5071333.

[17] I. Bramhecha, J. Sheikh, Development of sustainable citric acid-based polyol to synthesize waterborne polyurethane for antibacterial and breathable waterproof coating of cotton fabric, Ind. Eng. Chem. Res. 58 (2019) 21252–21261, https://doi.org/10.1021/acs.iecr.9b05195.

[18] C. Zhang, S. Bhoyate, M. Ionescu, P.K. Kahol, R.K. Gupta, Highly flame retardant and bio-based rigid polyurethane foams derived from orange peel oil, Polym. Eng. Sci. 58 (2018) 2078–2087, https://doi.org/10.1002/pen.24819.

[19] D. Kimmer, M. Kovarova, M. Yasir, L. Lovecka, J. Cisar, L. Musilova, J. Osicka, V. Sedlařík, Reinforced fluorinated copolymer and polyurethane electrospun layered nanofiber-based membranes for effective model water dead-end microfiltration, Polymers Adv. Techs 36 (2025) e70203, https://doi.org/10.1002/pat.70203.

[20] S. Gogoi, N. Karak, Biobased biodegradable waterborne hyperbranched polyurethane as an ecofriendly sustainable material, ACS Sustainable Chem. Eng. 2 (2014) 2730–2738, https://doi.org/10.1021/sc5006022.

[21] L. Lovecká, M. Kovářová, D. Hanušová, D. Kimmer, A. Poláchová, V. Sedlařík, Application of green solvents as a replacement of toxic dimethylformamide in the polylactic acid electrospinning process, Sustain. Mater. Technol. 44 (2025) e01405, https://doi.org/10.1016/j.susmat.2025.e01405.

[22] M. Ruan, H. Luan, G. Wang, M. Shen, Bio-polyols synthesized from bio-based 1,3-propanediol and applications on polyurethane reactive hot melt adhesives, Ind. Crop. Prod. 128 (2019) 436–444, https://doi.org/10.1016/j.indcrop.2018.11.045.

[23] M.A. Harmer, D.C. Confer, C.K. Hoffman, S.C. Jackson, A.Y. Liauw, A.R. Minter, E. R. Murphy, R.E. Spence, H.B. Sunkara, Renewably sourced polytrimethylene ether glycol by superacid catalyzed condensation of 1,3-propanediol, Green Chem. 12 (2010) 1410–1416, https://doi.org/10.1039/C002443K.

[24] C.E. McGlade, A review of the uncertainties in estimates of global oil resources, Energy 47 (2012) 262–270, https://doi.org/10.1016/j.energy.2012.07.048.

[25] J.P.S. Aniceto, I. Portugal, C.M. Silva, Biomass-based polyols through oxypropylation reaction, ChemSusChem 5 (2012) 1358–1368, https://doi.org/10.1002/cssc.201200032.

[26] B. Ahvazi, O. Wojciechowicz, T.-M. Ton-That, J. Hawari, Preparation of lignopolyols from wheat straw soda lignin, J. Agric. Food Chem. 59 (2011) 10505–10516, https://doi.org/10.1021/jf202452m.

[27] W. Chen, L. Zhong, X. Peng, R. Sun, F. Lu, Chemical fixation of carbon dioxide using a green and efficient catalytic system based on sugarcane bagasse—an agricultural waste, ACS Sustainable Chem. Eng. 3 (2015) 147–152, https://doi.org/10.1021/sc5006445.

[28] E.F. Gómez, X. Luo, C. Li, F.C. Michel, Y. Li, Biodegradability of crude glycerol-based polyurethane foams during composting, anaerobic digestion and soil incubation, Polym. Degrad. Stabil. 102 (2014) 195–203, https://doi.org/10.1016/j.polymdegradstab.2014.01.008.

[29] U.A. Amran, S. Zakaria, C.H. Chia, Z. Fang, M.Z. Masli, Production of liquefied oil palm empty fruit bunch based polyols via microwave heating, Energy Fuels 31 (2017) 10975–10982, https://doi.org/10.1021/acs.energyfuels.7b02098.

[30] L. Hojabri, X. Kong, S.S. Narine, Fatty acid-derived diisocyanate and biobased polyurethane produced from vegetable oil: synthesis, polymerization, and

characterization, Biomacromolecules 10 (2009) 884–891, https://doi.org/10.1021/bm801411w.
[31] G. Lligadas, J.C. Ronda, M. Galià, V. Cádiz, Plant oils as platform chemicals for polyurethane synthesis: current state-of-the-art, Biomacromolecules 11 (2010) 2825–2835, https://doi.org/10.1021/bm100839x.
[32] L. Serrano, M.G. Alriols, R. Briones, I. Mondragón, J. Labidi, Oxypropylation of rapeseed cake residue generated in the biodiesel production process, Ind. Eng. Chem. Res. 49 (2010) 1526–1529, https://doi.org/10.1021/ie9016732.
[33] S. Desai, J. Patel, V. Sinha, Polyurethane adhesive system from biomaterial-based polyol for bonding wood, Int. J. Adhesion Adhes. 23 (2003) 393–399, https://doi.org/10.1016/S0143-7496(03)00070-8.
[34] A. Llevot, P.-K. Dannecker, M. von Czapiewski, L.C. Over, Z. Söyler, M.A.R. Meier, Renewability is not enough: recent advances in the sustainable synthesis of biomass-derived monomers and polymers, Chem. Eur J. 22 (2016) 11510–11521, https://doi.org/10.1002/chem.201602068.
[35] H. Gang, D. Lee, K.-Y. Choi, H.-N. Kim, H. Ryu, D.-S. Lee, B.-G. Kim, Development of high performance polyurethane elastomers using vanillin-based green polyol chain extender originating from lignocellulosic biomass, ACS Sustainable Chem. Eng. 5 (2017) 4582–4588, https://doi.org/10.1021/acssuschemeng.6b02960.
[36] O. Kreye, H. Mutlu, M.A.R. Meier, Sustainable routes to polyurethane precursors, Green Chem. 15 (2013) 1431–1455, https://doi.org/10.1039/C3GC40440D.
[37] H. Li, J.-T. Sun, C. Wang, S. Liu, D. Yuan, X. Zhou, J. Tan, L. Stubbs, C. He, High modulus, strength, and toughness polyurethane elastomer based on unmodified lignin, ACS Sustainable Chem. Eng. 5 (2017) 7942–7949, https://doi.org/10.1021/acssuschemeng.7b01481.
[38] W. Liu, T. Xie, R. Qiu, Biobased thermosets prepared from rigid isosorbide and flexible soybean oil derivatives, ACS Sustainable Chem. Eng. 5 (2017) 774–783, https://doi.org/10.1021/acssuschemeng.6b02117.
[39] D. Tang, B.A.J. Noordover, R.J. Sablong, C.E. Koning, Metal-free synthesis of novel biobased dihydroxyl-terminated aliphatic polyesters as building blocks for thermoplastic polyurethanes, J. Polym. Sci. Polym. Chem. 49 (2011) 2959–2968, https://doi.org/10.1002/pola.24732.
[40] M. Burelo, I. Gaytán, H. Loza-Tavera, J.A. Cruz-Morales, D. Zárate-Saldaña, M. J. Cruz-Gómez, S. Gutiérrez, Synthesis, characterization and biodegradation studies of polyurethanes: effect of unsaturation on biodegradability, Chemosphere 307 (2022) 136136, https://doi.org/10.1016/j.chemosphere.2022.136136.
[41] K. Błażek, J. Datta, Renewable natural resources as green alternative substrates to obtain bio-based non-isocyanate polyurethanes-review, Crit. Rev. Environ. Sci. Technol. 49 (2019) 173–211, https://doi.org/10.1080/10643389.2018.1537741.
[42] Y. Ma, Y. Xiao, Y. Zhao, Y. Bei, L. Hu, Y. Zhou, P. Jia, Biomass based polyols and biomass based polyurethane materials as a route towards sustainability, React. Funct. Polym. 175 (2022) 105285, https://doi.org/10.1016/j.reactfunctpolym.2022.105285.
[43] D. Kimmer, M. Zatloukal, D. Petras, I. Vincent, P. Slobodian, Investigation of Polyurethane Electrospinning Process Efficiency, AIP Publishing LLC, Melville, New York, USA, 2009, pp. 305–311.
[44] R. Xu, J. Feng, L. Zhang, S. Li, Low viscosity of spinning liquid to prepare organic-inorganic hybrid ultrafine nanofiber membrane for high-efficiency filtration application, Separ. Purif. Technol. 303 (2022) 122224, https://doi.org/10.1016/j.seppur.2022.122224.
[45] H. Liu, Y. Zhu, C. Zhang, Y. Zhou, D.-G. Yu, Electrospun nanofiber as building blocks for high-performance air filter: a review, Nano Today 55 (2024) 102161, https://doi.org/10.1016/j.nantod.2024.102161.
[46] D. Kimmer, I. Vincent, L. Lovecka, T. Kazda, A. Giurg, O. Skorvan, Some aspects of applying nanostructured materials in air filtration, water filtration and electrical engineering, AIP Conf. Proc. 1843 (2017) 060001, https://doi.org/10.1063/1.4983003.
[47] T. Lu, J. Cui, Q. Qu, Y. Wang, J. Zhang, R. Xiong, W. Ma, C. Huang, Multistructured electrospun nanofibers for air filtration: a review, ACS Appl. Mater. Interfaces 13 (2021) 23293–23313, https://doi.org/10.1021/acsami.1c06520.
[48] D. Kimmer, I. Vincent, W. Sambaer, M. Zatloukal, J. Ondracek, Modeling and Preparation of Nanofibre and Composite Nanostructures, AIP Publishing LLC, Melville, New York, USA, 2015, https://doi.org/10.1063/1.4918869, 050001-1-050001–6.
[49] W. Sambaer, M. Zatloukal, D. Kimmer, 3D air filtration modeling for nanofiber based filters in the ultrafine particle size range, Chem. Eng. Sci. 82 (2012) 299–311, https://doi.org/10.1016/j.ces.2012.07.031.
[50] D. Kimmer, I. Vincent, J. Fenyk, D. Petras, M. Zatloukal, W. Sambaer, V. Zdimal, M. Zatloukal, Morphology of nano and micro fiber structures in ultrafine particles filtration, in: Zlin, Czech Republic, 2011, pp. 295–311, https://doi.org/10.1063/1.3604490.
[51] W. Sambaer, M. Zatloukal, D. Kimmer, The use of novel digital image analysis technique and rheological tools to characterize nanofiber nonwovens, Polym. Test. 29 (2010) 82–94, https://doi.org/10.1016/j.polymertesting.2009.09.008.
[52] Z. Sarac, A. Kilic, C. Tasdelen-Yucedag, Optimization of electro-blown polysulfone nanofiber mats for air filtration applications, Polym. Eng. Sci. 63 (2023) 723–737, https://doi.org/10.1002/pen.26236.
[53] W. Sambaer, M. Zatloukal, D. Kimmer, 3D modeling of filtration process via polyurethane nanofiber based nonwoven filters prepared by electrospinning process, Chem. Eng. Sci. 66 (2011) 613–623, https://doi.org/10.1016/j.ces.2010.10.035.
[54] T.T. Bui, M.K. Shin, S.Y. Jee, D.X. Long, J. Hong, M.-G. Kim, Ferroelectric PVDF nanofiber membrane for high-efficiency PM0.3 air filtration with low air flow resistance, Colloids Surf. A Physicochem. Eng. Asp. 640 (2022) 128418, https://doi.org/10.1016/j.colsurfa.2022.128418.
[55] C. Liu, P.-C. Hsu, H.-W. Lee, M. Ye, G. Zheng, N. Liu, W. Li, Y. Cui, Transparent air filter for high-efficiency PM2.5 capture, Nat. Commun. 6 (2015) 6205, https://doi.org/10.1038/ncomms7205.
[56] J.J. Huang, Y. Tian, R. Wang, M. Tian, Y. Liao, Fabrication of bead-on-string polyacrylonitrile nanofibrous air filters with superior filtration efficiency and ultralow pressure drop, Separ. Purif. Technol. 237 (2020) 116377, https://doi.org/10.1016/j.seppur.2019.116377.
[57] H. Wan, N. Wang, J. Yang, Y. Si, K. Chen, B. Ding, G. Sun, M. El-Newehy, S.S. Al-Deyab, J. Yu, Hierarchically structured polysulfone/titania fibrous membranes with enhanced air filtration performance, J. Colloid Interface Sci. 417 (2014) 18–26, https://doi.org/10.1016/j.jcis.2013.11.009.
[58] Y. Bian, S. Wang, L. Zhang, C. Chen, Influence of fiber diameter, filter thickness, and packing density on PM2.5 removal efficiency of electrospun nanofiber air filters for indoor applications, Build. Environ. 170 (2020) 106628, https://doi.org/10.1016/j.buildenv.2019.106628.
[59] B. Liu, S. Zhang, X. Wang, J. Yu, B. Ding, Efficient and reusable polyamide-56 nanofiber/nets membrane with bimodal structures for air filtration, J. Colloid Interface Sci. 457 (2015) 203–211, https://doi.org/10.1016/j.jcis.2015.07.019.
[60] D. Kowalczuk, M. Pitucha, Application of FTIR method for the assessment of immobilization of active substances in the matrix of biomedical materials, Materials 12 (2019) 2972, https://doi.org/10.3390/ma12182972.
[61] I.D. dos Santos Silva, A. Albuquerque, L. Boskamp, A. Ries, K. Haag, K. Koschek, R. Wellen, Synthesis of bio-polyurethanes with isosorbide and propanediol based poly(lactic acid) diol, J. Appl. Polym. Sci. 140 (2023) e53623, https://doi.org/10.1002/app.53623.
[62] B. Quienne, N. Kasmi, R. Dieden, S. Caillol, Y. Habibi, Isocyanate-free fully biobased star polyester-urethanes: synthesis and thermal properties, Biomacromolecules 21 (2020) 1943–1951, https://doi.org/10.1021/acs.biomac.0c00156.
[63] P. Somdee, T. Lassú-Kuknyó, C. Kónya, T. Szabó, K. Marossy, Thermal analysis of polyurethane elastomers matrix with different chain extender contents for thermal conductive application, J. Therm. Anal. Calorim. 138 (2019) 1003–1010, https://doi.org/10.1007/s10973-019-08183-y.
[64] B. Pukánszky Jr., K. Bagdi, Z. Tóvölgyi, J. Varga, L. Botz, S. Hudak, T. Dóczi, B. Pukánszky, Effect of interactions, molecular and phase structure on the properties of polyurethane elastomers, in: Z.D. Hórvölgyi, É. Kiss (Eds.), Colloids for Nano- and Biotechnology, Springer Berlin Heidelberg, Berlin, Heidelberg, 2008, pp. 218–224, https://doi.org/10.1007/2882_2008_102.
[65] M. Abiad, M. Carvajal, O. Campanella, A review on methods and theories to describe the glass transition phenomenon: applications in food and pharmaceutical products, Food Eng. Rev. 1 (2009) 105–132, https://doi.org/10.1007/s12393-009-9009-1.
[66] W.C. Hinds, Aerosol Technology, Properties, Behavior, and Measurement of Airborne Particles, second ed., JOHN WILEY & SONS, New York, n.d.